Hydrodynamic structure of a bubbly flow in an annular channel: experimental study by means of PIV/PFBI/PTV

P D Lobanov[1] and M V Timoshevskiy[1,2]

[1] Kutateladze Institute of Thermophysics, Siberian Branch of the Russian Academy of Sciences, 1, Lavrentyev Ave., Novosibirsk, 630090, Russia
[2] Department of Physics, Novosibirsk State University, 2, Pirogov Str., Novosibirsk, 630090, Russia

lobanov@itp.nsc.ru

Abstract. In the paper, an experimental investigation of the local structure of a bubbly upward flow in an annular channel was carried out by means of a combination of PIV/PFBI/PTV techniques. PIV was applied to measure velocity distributions and turbulent characteristics in the continuous phase, PFBI approach was applied to visualize bubbles in the flow and evaluate their positions and sizes and the simplest PTV method was employed to determine the bubble velocities. The flow was studied at the Reynolds number of 12,500 and different void fractions β = 0, 1 and 2%. The mean air bubble diameter was estimated to be about 0.8 mm for all β. Bubble concentration was observed to increase near the channel walls. Rising velocity of the gas bubbles was measured in various locations across the annulus duct and it was found that it is substantially higher for the bubbles moving in the central part of the channel. An increase of the void fraction resulted in redistribution of the mean velocity in the flow cross-section and intensification of the turbulent fluctuations up to three times for β = 2%.

1. Introduction

Two-phase bubbly flows are used in various hydrotechnical and hydropower engineering facilities, which makes their investigation vitally important and highly urgent. In most of the studies on the heat transfer and hydrodynamics in bubbly media available in literature at present, high-Reynolds-number dispersed flows in vertical pipes are mainly considered (e.g. [1–5]). Depending on the gas concentration, size distribution of bubbles, Reynolds number, characteristic turbulence scales and other conditions, various effects can be observed. For instance, injection of a gas into a moving liquid is well known [6, 7] to cause a noticeable modification of the flow hydrodynamic structure (even at low gas fractions) due to redistribution of gas bubbles across a duct and, thereby, alteration of the mean flow and intensification or suppression of turbulence, e.g. this phenomenon is determinative for heat transfer processes in the near-wall region.

In spite of the fact that the literature is abundant in researches on bubbly pipe flows, it lacks for experimental studies on bubbly flows in complex geometries, such as annular channels, vertical rod assemblies, tubes with partially obscured cross-section and others. Moreover, results obtained for a pipe flow can be hardly translated to a complicated flow which seem, however, quite similar at first glance, e.g. annular flow where liquid moves through a gap between two coaxial tubes. Annular channel is a simplified test object for modeling the flow in fuel assemblies of nuclear power units. Presently, there are only a small number of papers dealing with this topic in the literature. As an

example, Ozar et al. [8] measured dispersed phase characteristics (local gas fraction, specific interfacial area and phase slip velocity) but the mean and turbulent characteristics of the continuous phase left undetermined. All these imply the investigation of bubbly flows in annular channels is of a high importance.

Probably, the most crucial problem that one faces when studying a bubbly flow is the choice of measurement techniques. Among a large number of different approaches for two-phase media diagnostics, two main categories are distinguished: intrusive and contactless. All contact methods allow only point measurements of various flow characteristics and most of them have a high temporal resolution. In an overwhelming majority of the researches, right intrusive techniques are conventionally applied. Non-intrusive methods are, as a rule, optical and are conversely employed to visualize or measure instantaneous spatial distributions of certain quantities within a flow region of interest but their temporal resolution is relatively low, except for LDA and PDA. The principal limitation of all optical approaches is that they can be applied only when the bubble density is sufficiently low (commonly at void factions of about 1%). Nevertheless, during the last two decades the optical methods have been developed considerably and are now utilized more and more frequently, with their temporal resolution increasing progressively. This makes their use nowadays more preferable and profitable.

In the paper, a bubbly upward flow in an annular channel is studied experimentally at the same Re = 12,500 for several gas volume fractions β = 0, 1, 2% and the same bubble size by means of a combination of high-speed particle image velocimetry and planar fluorescence for bubbles imaging – PFBI (see [9, 10]) approaches. We report here on a visual analysis of high-speed images registered by a shadow photography (SP) and PFBI techniques to determine the mean bubble size, their velocities and distributions across the annular flow, as well as on PIV measurements of spatial distributions of instantaneous velocity inside the annulus, with a special emphasis put on the effect of dispersed phase on the flow mean velocity and turbulent fluctuations profiles.

2. Experiment

The bubbly annular flow was reproduced in the hydrodynamic rig in Kutateladze Institute of Thermophysics SB RAS. The experimental setup is of closed type and continuous operation. Its test channel is formed by two concentric tubes of roughly 2.7 m height made of transparent organic glass. The internal tube is constituted from three aligned sections with the outer diameter of D_{INT} = 20 mm, while the external one is composed of five in-line parts with the inner diameter of D_{EXT} = 42.2 mm. So, the hydraulic diameter of the annular channel is equal to D_H = 22.2 mm. The inlet of the test section equipped with an immersion unit filled with quiescent distilled water to reduce optical distortions is located at the distance of $70D_H$ from the annulus inlet for hydrodynamic stabilization of the flow (see Fig. 1). The distance from the test section outlet to the annulus outlet is $35D_H$ to minimize the influence of downstream transformation of the pipeline, which can cause flow separation, acceleration, bending, vortex generation and so on.

The operating fluid was also distilled water which was driven by a centrifugal pump equipped with a control module to vary the rotor speed. The flow rate was measured by an ultrasonic flowmeter. The water temperature was maintained constant at 30±0.1 °C in the test section by means of a thermostatic regulator filled with tap water as a heat-transfer agent and containing a tubular electrical heater, cooling circuit and aquarium pump to permanently blend the heat carrier. Cooling and heating in the thermostat was implemented by a PID-control system activating an electromagnetic valve to start/stop the coolant supply to the cooling circuit and a switching relay to loop/break the electric line to the heater. The liquid temperature was measured by heat-variable resistors placed in the test section, heat exchanger and settling tank. The Reynolds number based on the superficial liquid velocity $V_0 = 4 \cdot Q_W/[\pi \cdot (D_{EXT}^2 - D_{INT}^2)]$ = 0.45 m/s, where Q_W is the water volume rate (measurement error is 2%), and D_H equaled approximately to 12,500.

In order to saturate the flow with bubbles, an air-water mixer of a special design was used to provide a quasi-monodisperse size distribution of the bubbles. The air was supplied to the mixer by a

compressor through a couple of filters of rough (5 μm) and fine (0.01 μm) cleaning. The air overpressure at the mixer inlet was specified in the range of 9.8–19.6 kPa depending on the air volume flow rate Q_A by a high-precision reducer. The air temperature, pressure and flow rate were measured together by a thermal mass flowmeter (TSI model 4140) with the measurement uncertainties 0.1 °C, 0.1 kPa and 2%, respectively. Different volume gas fractions $\beta = Q_A/(Q_W+Q_A)$ in the annular flow were achieved by changing Q_A using a needle valve. In experiments, β possessed the following values: 0, 1 and 2%. The mean diameter of the bubbles D_B was approximately 0.8 mm for all β.

Figure 1. A photograph of the test section of the annular channel with the immersion unit filled with distilled water. Fragments of the laser head and camera lens are also visible in the picture, which displays the arrangement of the measurement system.

For the implementation of PFBI approach (which details are given in [9, 10]) to visualize bubbles in the flow, the water was merged with Rhodamine 6G as a fluorescent dye, the concentration of which was relatively low (about 86 μg/l). So, the water properties, especially viscosity and surface tension, can be considered unchanged. As bubbles illuminated by a laser light produce bright glares in images and, thereby, contaminate raw data, a laser-induced fluorescence (LIF) approach was applied to avoid their undesirable effect on PIV measurements. For this, fluorescent seeding particles made of polymethyl methacrylate filled with Rhodamine B of MicroParticles GmbH production (hydrophobic, size distribution 1–20 μm, wavelength range 550–700 nm) were added into the operating liquid to perform PIV measurements.

In order to illuminate and register the bubbles and tracers suspended in the flow, a PIV-system with a high temporal resolution consisting of a pulsed Nd:YAG Photonics Industries DM-532-50 laser (wavelength 532 nm, repetition rate 15 kHz, pulse duration 10 ns, pulse energy 15 mJ), Photron FASTCAM SA5 CMOS-camera (digit capacity 12 bits, resolution 1,024x1,024 pix., acquisition rate 7 kHz) equipped with a Sigma DG Macro 105 mm f/2.8D lens, a system of extension rings of 116 mm cumulative length and a low-pass optical filter (transmission edge at 570 nm) and Berkeley Nucleonics Corporation pulse/delay generator (model 575) for external synchronization was employed (Fig. 1). The distance between the camera and the measurement plane was roughly 395 mm. The magnification of the optical system was 1.8, which allowed us to reduce the plane dimensions of the measurement region approximately to 11.5x11.5 mm. The thickness of a laser light sheet was about 1 mm in the measurement section that passed through the annulus axis. In the experiment, the recording rate was 5 kHz.

The raw data (a series of 10,000 PFBI snapshots for each regime) gathered continuously during 2 seconds were processed using a PC with “ActualFlow” software [11]. At first, two procedures, namely subtraction of the mean two-frame intensity field averaged over the whole sample range and masking, were successively applied to enhance the quality of the registered images and to remove the areas corresponding to shadows from the subsequent calculations. Velocity fields were calculated using the iterative cross-correlation algorithm with a continuous window shift and deformation and 75% overlap of the interrogation windows. In addition, at this step of processing the local particle concentration was accounted for. In order to have a relatively large dynamic range, the initial size of the interrogation window was chosen to be 64x64 pixels but it was subsequently reduced so that the final interrogation window was 8x8 pixels, which provided a high enough spatial resolution. The obtained instantaneous velocity vector fields were then validated with the following procedures: peak validation

with the threshold of 2.0, adaptive median 7x7 filter and cluster validation with the coefficient of 50 [12].

3. Results

Results of the bubbly flow visualization by both SP and PFBI are shown together for different void fractions in Fig. 2 to facilitate a direct comparison between the methods. As seen, an analysis of the images is considerably complicated due to several reasons. First, both types of the images are noticeably distorted from the outer side (at the left) because of the annulus external tube curvature. Second, PFBI patterns of the bubbles located close to the channel walls are partial (Fig. 2-b) because, in the experiment, these bubbles are not illuminated by the fluorescent dye emission from the side of both internal and external tubes, so automated identification of such bubbles is extremely difficult. Further, out-of-focus bubbles corresponding to dark blurred regions in the PFBI images (Fig. 2-b) and spatially situated in front of the measurement section often overlap in-focus bubbles with sharp bright borders. This can result in an underestimation of the local gas fraction and an increase of its measurement uncertainty, especially in the near-wall region at higher β. Finally, the bubble and tracer patterns are substantially merged (Fig. 2-b), which makes it difficult to distinguish the signals from the dispersed and continuous phases and, thereby, correctly calculate the mean velocity and turbulent characteristics in the flow.

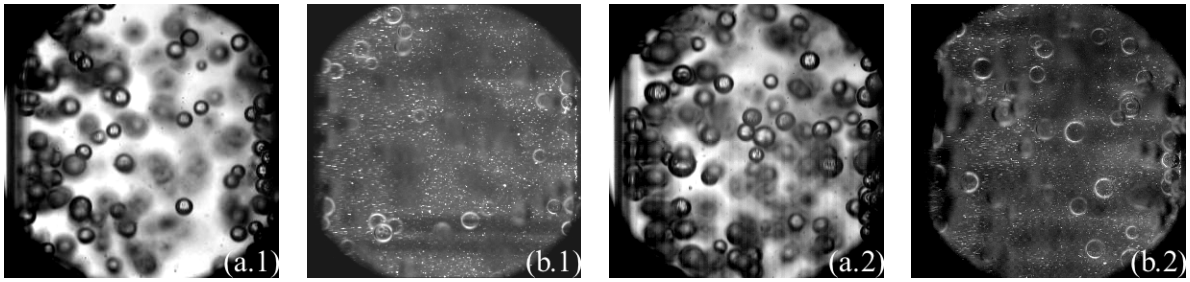

Figure 2. Examples of instantaneous images of the bubbly annular flow captured by (a) shadow photography and (b) PFBI approach for (1) β = 1% and (2) β = 2%. The external wall of the annular channel is at the left-hand side of the images, while the inner one is at the right. In case of PFBI, bright spots correspond to seeding particles used for PIV measurements.

Figure 2 also demonstrates that the bubble shape is spherical. The mean bubble size was estimated to be roughly D_B = 0.8 mm. Most of the bubbles were found to move close to the annular channel walls rather than in its central part, which is connected with the balance of forces acting on the bubbles in the flow. This implies that the profile of the local gas concentration across the annulus is saddle-shaped. According to [1-3], such a trend is typical for upward pipe flows containing small bubbles. A saddle-shaped profile can cause a redistribution of local characteristics in a two-phase flow in comparison with those for the single-phase flow and, thereby, change heat- and mass-transfer parameters of the flow [2]. In order to recognize bubbles in the PFBI images, a correlation-based algorithm [9] was used. This processing procedure divides a bubble pattern into several sectors and calculates the correlation coefficient between a part of raw PFBI image and a corresponding one of a 2D Gaussian mask independently for each of the sectors and, thus, allows an identification of overlapped and partially illuminated bubble patterns. Its output is positions of bubble centers and their radii. Analyzing the shift between bubble positions in successive images, it is possible to evaluate its instantaneous velocity (the simplest PTV approach).

Time variation of the measured bubble velocities in the annular upward flow is presented in Fig. 3. For this, all the bubbles were divided into three categories depending on their transverse coordinate: located in the central part of the channel and near the internal and external walls, using the criterion of $0.2 < x/L < 0.8$ for the central region, where $L = (D_{EXT}–D_{INT})/2$ = 11.1 mm. The bubble velocity is observed to change in time by maximum 40% (Fig. 3). For approximation, the mean velocity of the bubbles moving in the central part was also calculated with the following formula [13]:

$$V_B = C \cdot V_0 + V_T, \quad (1)$$

where V_B is the measured bubble velocity in the two-phase annular flow, C is a proportionality coefficient equaled to 1.2 [13], V_T = 0.09 m/s is the terminal velocity of an air bubble rising in a quiescent water. As seen (Fig. 3), this approximation is in a good agreement with the measurements. It is worth noting that such a trend is common for all bubbles moving in the central part of the annulus. Thus, this value of C = 1.2 can be recommended for the drift-flux model under conditions similar to the present ones.

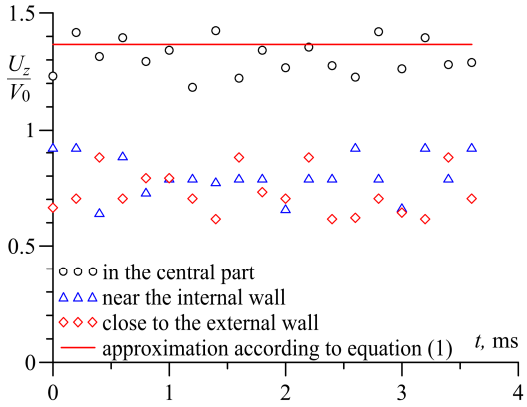

Figure 3. Time dependence of the rising velocity of air bubbles in different locations across the annulus (β = 1%). The estimation of the bubble velocity in each location was based on consideration of only one bubble.

In the central part of the annulus, the mean liquid velocity is equal to about 1.2 for all β (see Fig. 4-a), which is characteristic for turbulent fluid motion in channels. Unlike the case of fluid motion in axisymmetric pipes, the velocity maximum of the single-phase annular flow is not at the duct center but somewhat (x/L = 0.461) shifted to its inner wall. Turbulent fluctuations are in the range of 0.06–0.08V_0 in the central part of the annular channel and gradually grow up to 0.18V_0 when approaching the walls (Fig. 4-b). An increase of the volume gas fraction leads to a further displacement of the mean velocity maximum to the internal wall (Fig. 4-a), so that it is located at x/L = 0.425 and 0.387 for β = 1 and 2%, respectively. Turbulence intensity rises across the whole annulus duct when the volume gas fraction increases. For β = 2%, it reaches 0.12V_0 in the central flow region and $\tilde{v}_z/V_0$ = 0.28–0.3 near the walls (Fig. 4-b). Moreover, the transverse dimension of the near-wall region where turbulent fluctuations are high is several times larger for the external wall (0.1L) compared to the internal one (about 0.02L).

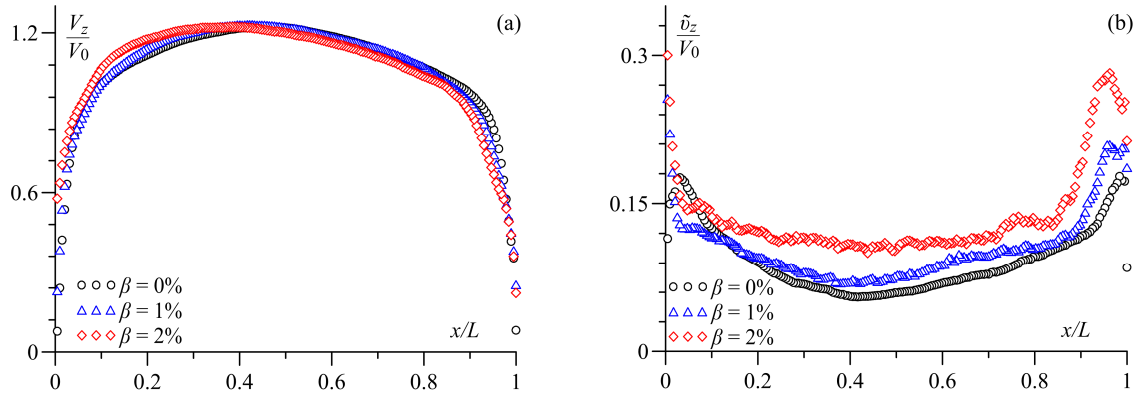

Figure 4. Profiles of the longitudinal component of (a) the mean velocity and (b) its turbulent fluctuations (r.m.s. values) of the continuous phase in the annulus cross-section for different void fractions. z- and x-axes are directed downstream and crosswise. The internal and external walls of the annulus are located at x/L = 0 and 1, respectively. Only every fifth measured point is shown.

4. Summary

The bubbly annular upward flow with void fractions up to β = 2% and the mean bubble size equal to 0.8 mm was for the first time studied by a combination of PIV/PFBI/PTV approaches at the Reynolds number Re = 12,500. Under such conditions, the air bubbles were found to tend to migrate to the near-wall regions. Bubble velocities are higher in the central part of the annulus compared to those in the near-wall regions. An increase of the volume gas fraction results in redistribution of the mean velocity across the channel so that its maximum shifts to the inner wall and intensification of turbulent fluctuations over the whole channel cross-section up to two or three times for β = 2%.

Acknowledgments

The experimental study was financially supported by a grant from the Russian Foundation for Basic Research (Project No. 15-38-21040-mol_a_ved supervised by PhD P. Lobanov).

References

[1] Serizawa A, Kataoka I and Michiyoshi I 1975 Turbulence structure of air-water bubbly flow – II. Local properties *Int. J. Multiphase Flow* **2** 235–46

[2] Nakoryakov V E, Kashinsky O N, Burdukov A P and Odnoral V P 1981 Local characteristics of upward gas-liquid flows *Int. J. Multiphase Flow* **7** 63–81

[3] Wang S K, Lee S J, Jones Jr O C and Lahey Jr R T 1987 3-D turbulence structure and phase distribution measurements in bubbly two-phase flows *Int. J. Multiphase Flow* **13** 327–43

[4] Kashinsky O N and Randin V V 1999 Downward bubbly gas-liquid flow in a vertical pipe *Int. J. Multiphase Flow* **25** 109–38

[5] Hibiki T, Ishii M and Xiao Z 2001 Axial interfacial area transport of vertical bubbly flows *Int. J. Heat Mass Transfer* **44** 1869–88

[6] Kashinsky O N, Lobanov P D, Pakhomov M A, Randin V V and Terekhov V I 2006 Experimental and numerical study of downward bubbly flow in a pipe *Int. J. Heat Mass Transfer* **49** 3717–27

[7] Lu J and Tryggvason G 2007 Effect of bubble size in turbulent bubbly downflow in a vertical channel *Chem. Eng. Sci.* **62** 3008–18

[8] Ozar B, Jeong J J, Dixit A, Juliá J E, Hibiki T and Ishii M 2008 Flow structure of gas-liquid two-phase flow in an annulus *Chem. Eng. Sci.* **63** 3998–4011

[9] Akhmetbekov Ye K, Alekseenko S V, Dulin V M, Markovich D M and Pervunin K S 2010 Planar fluorescence for round bubble imaging and its application for the study of an axisymmetric two-phase jet *Exp. Fluids* **48(4)** 615–29

[10] Dulin V M, Markovich D M and Pervunin K S 2012 The optical principles of PFBI approach *AIP Conf. Proc.* **1428** 217–24

[11] Akhmetbekov Ye K, Bilsky A V, Lozhkin Yu A, Markovich D M, Tokarev M P and Tyuryushkin A N 2006 Software for experiment management and processing of data obtained by digital flow visualization techniques (ActualFlow) *Numer. Methods Program.* **7** 79–85 (in Russian)

[12] Kravtsova A Yu, Markovich D M, Pervunin K S, Timoshevskiy M V and Hanjalić K 2014 High-speed visualization and PIV measurements of cavitating flows around a semi-circular leading-edge flat plate and NACA0015 hydrofoil *Int. J. Multiphase Flow* **60** 119–134

[13] Nicklin D J 1962 Two-phase bubble flow *Chem. Eng. Sci.* **17** 693–702